References

1. Oda E, Kawai R, Watanabe K, Sukumaran V. Prevalence of metabolic syndrome increases with the increase in blood levels of gamma glutamyltransferase and alanine aminotransferase in Japanese men and women. Intern Med **48**: 1343-1350, 2009.
2. Lee DS, Evans JC, Robins SJ, et al. Gamma glutamyl transferase and metabolic syndrome, cardiovascular disease, and mortality risk: the Framingham Heart Study. Arterioscler Thromb Vasc Biol **27**: 127-133, 2007.
3. Meisinger C, Döring A, Schneider A, Löwel H; KORA Study Group. Serum gamma-glutamyltransferase is a predictor of incident coronary events in apparently healthy men from the general population. Atherosclerosis **189**: 297-302, 2006.
4. Schindhelm RK, Dekker JM, Nijpels G, et al. Alanine aminotransferase predicts coronary heart disease events: a 10-year follow-up of the Hoorn Study. Atherosclerosis **191**: 391-396, 2007.
5. Devers MC, Campbell S, Shaw J, Zimmet P, Simmons D. Should liver function tests be included in definitions of metabolic syndrome? Evidence from the association between liver function tests, components of metabolic syndrome and prevalent cardiovascular disease. Diabet Med **25**: 523-529, 2008.
6. Adams LA, Waters OR, Knuiman MW, Elliott RR, Olynyk JK. NAFLD as a risk factor for the development of diabetes and the metabolic syndrome: an eleven-year follow-up study. Am J Gastroenterol **104**: 861-867, 2009.
7. André P, Balkau B, Vol S, Charles MA, Eschwège E; DESIR Study Group. Gamma-glutamyltransferase activity and development of the metabolic syndrome (International Diabetes Federation Definition) in middle-aged men and women: Data from the Epidemiological Study on the Insulin Resistance Syndrome (DESIR) cohort. Diabetes Care **30**: 2355-2361, 2007.
8. Sakurai M, Takamura T, Ota T, et al. Liver steatosis, but not fibrosis, is associated with insulin resistance in nonalcoholic fatty liver disease. J Gastroenterol **42**: 312-317, 2006.
9. Targher G, Arcaro G. Non-alcoholic fatty liver disease and increased risk of cardiovascular disease. Atherosclerosis **191**: 235-240, 2007.
10. McKimmie RL, Daniel KR, Carr JJ, et al. Hepatic steatosis and subclinical cardiovascular disease in a cohort enriched for type 2 diabetes: the Diabetes Heart Study. Am J Gastroenterol **103**: 3029-3035, 2008.
11. McCullough AJ. The epidemiology and risk factors of NASH. In: Fatty Liver Disease: NASH and Related Disorders. Farrell GC, George J, de la M Hall P, McCullough AJ, Eds. Blackwell Publishing, Malden, MA, 2005: 23-37.
12. Weston SR, Leyden W, Murphy R, et al. Racial and ethnic distribution of nonalcoholic fatty liver in persons with newly diagnosed chronic liver disease. Hepatology **41**: 372-379, 2005.
13. Amarapurkar DN, Hashimoto E, Lesmana LA, Sollano JD, Chen PJ, Goh KL; Asia-Pacific Working Party on NAFLD. How common is non-alcoholic fatty liver disease in the Asia-Pacific region and are there local differences? J Gastroenterol Hepatol **22**: 788-793, 2007.
14. Fan JG, Li F, Cai XB, Peng YD, Ao QH, Gao Y. Effects of nonalcoholic fatty liver disease on the development of metabolic disorders. J Gastroenterol Hepatol **22**: 1086-1091, 2007.

⌘ *Author's Choice*

THE JOURNAL OF BIOLOGICAL CHEMISTRY VOL. 284, NO. 22, pp. 14809–14818, May 29, 2009

Palmitate Induces Insulin Resistance in H4IIEC3 Hepatocytes through Reactive Oxygen Species Produced by Mitochondria*[S]

Received for publication, March 5, 2009 Published, JBC Papers in Press, March 30, 2009, DOI 10.1074/jbc.M901488200

Seiji Nakamura[‡], Toshinari Takamura[‡1], Naoto Matsuzawa-Nagata[§], Hiroaki Takayama[‡], Hirofumi Misu[‡], Hiroyo Noda[‡], Satoko Nabemoto[‡], Seiichiro Kurita[‡], Tsuguhito Ota[‡], Hitoshi Ando[‡], Ken-ichi Miyamoto[§], and Shuichi Kaneko[‡]

From the [‡]Department of Disease Control and Homeostasis, Kanazawa University Graduate School of Medical Science, and the [§]Department of Medicinal Informatics, Kanazawa University Hospital, 13-1 Takara-machi, Kanazawa 920-8641, Japan

Visceral adiposity in obesity causes excessive free fatty acid (FFA) flux into the liver via the portal vein and may cause fatty liver disease and hepatic insulin resistance. However, because animal models of insulin resistance induced by lipid infusion or a high fat diet are complex and may be accompanied by alterations not restricted to the liver, it is difficult to determine the contribution of FFAs to hepatic insulin resistance. Therefore, we treated H4IIEC3 cells, a rat hepatocyte cell line, with a monounsaturated fatty acid (oleate) and a saturated fatty acid (palmitate) to investigate the direct and initial effects of FFAs on hepatocytes. We show that palmitate, but not oleate, inhibited insulin-stimulated tyrosine phosphorylation of insulin receptor substrate 2 and serine phosphorylation of Akt, through c-Jun NH_2-terminal kinase (JNK) activation. Among the well established stimuli for JNK activation, reactive oxygen species (ROS) played a causal role in palmitate-induced JNK activation. In addition, etomoxir, an inhibitor of carnitine palmitoyltransferase-1, which is the rate-limiting enzyme in mitochondrial fatty acid β-oxidation, as well as inhibitors of the mitochondrial respiratory chain complex (thenoyltrifluoroacetone and carbonyl cyanide *m*-chlorophenylhydrazone) decreased palmitate-induced ROS production. Together, our findings in hepatocytes indicate that palmitate inhibited insulin signal transduction through JNK activation and that accelerated β-oxidation of palmitate caused excess electron flux in the mitochondrial respiratory chain, resulting in increased ROS generation. Thus, mitochondria-derived ROS induced by palmitate may be major contributors to JNK activation and cellular insulin resistance.

Insulin is the major hormone that inhibits gluconeogenesis in the liver. Visceral adiposity in obesity causes hepatic steatosis and insulin resistance. In an insulin-resistant state, impaired insulin action allows enhancement of glucose production in the liver, resulting in systemic hyperglycemia (1) and contributing to the development of type 2 diabetes. In addition, we have demonstrated experimentally that insulin resistance accelerated the pathology of steatohepatitis in genetically obese diabetic OLETF rats (2). In contrast, lipid-induced oxidative stress caused steatohepatitis and hepatic insulin resistance in mice (3). In fact, steatosis of the liver is an independent predictor of insulin resistance in patients with nonalcoholic fatty liver disease (4).

It remains unclear whether hepatic steatosis causally contributes to insulin resistance or whether it is merely a resulting pathology. Excessive dietary free fatty acid (FFA)[2] flux into the liver via the portal vein may cause fatty liver disease and hepatic insulin resistance. Indeed, elevated plasma FFA concentrations correlate with obesity and decreased target tissue insulin sensitivity (5).

Experimentally, lipid infusion or a high fat diet that increases circulating FFA levels promotes insulin resistance in the liver. Candidate events linking FFA to insulin resistance *in vivo* are the up-regulation of SREBP-1c (6), inflammation caused by activation of c-Jun amino-terminal kinase (JNK) (7) or IKKβ (8), endoplasmic reticulum (ER) stress (9), ceramide (10, 11), and TRB3 (12).

However, which event is the direct and initial target of FFA in the liver is unclear. Insulin resistance induced by lipid infusion or a high fat diet is complex and may be accompanied by alterations not restricted to the liver, making it difficult to determine the contribution of FFAs to hepatic insulin resistance. For example, hyperinsulinemia and hyperglycemia secondary to the initial event also may contribute to the development of diet-induced insulin resistance *in vivo* (6).

To address the early event(s) triggering the development of high fat diet- or obesity-induced insulin resistance, we investigated the molecular mechanism(s) underlying the direct action of FFA on hepatocytes to cause insulin resistance *in vitro*, using the rat hepatocyte cell line H4IIEC3. We found that mitochondria-derived reactive oxygen species (ROS) were a cause of palmitate-induced insulin resistance in hepatocytes.

* This work was supported by grants-in-aid from the Ministry of Education, Culture, Sports, Science, and Technology of Japan.
⌘ *Author's Choice*—Final version full access.
[S] The on-line version of this article (available at http://www.jbc.org) contains supplemental Figs. 1–8.
[1] To whom correspondence should be addressed. Tel.: 81-76-265-2233; Fax: 81-76-234-4250; E-mail: ttakamura@m-kanazawa.jp.

[2] The abbreviations used are: FFA, free fatty acid; IRS, insulin receptor substrate; JNK, c-Jun NH_2-terminal kinase; ER, endoplasmic reticulum; ROS, reactive oxygen species; NAC, *N*-acetyl-L-cysteine; H2DCFDA, 2′,7′-dichlorofluorescin diacetate; OXPHOS, oxidative phosphorylation; PVDF, polyvinylidene difluoride.

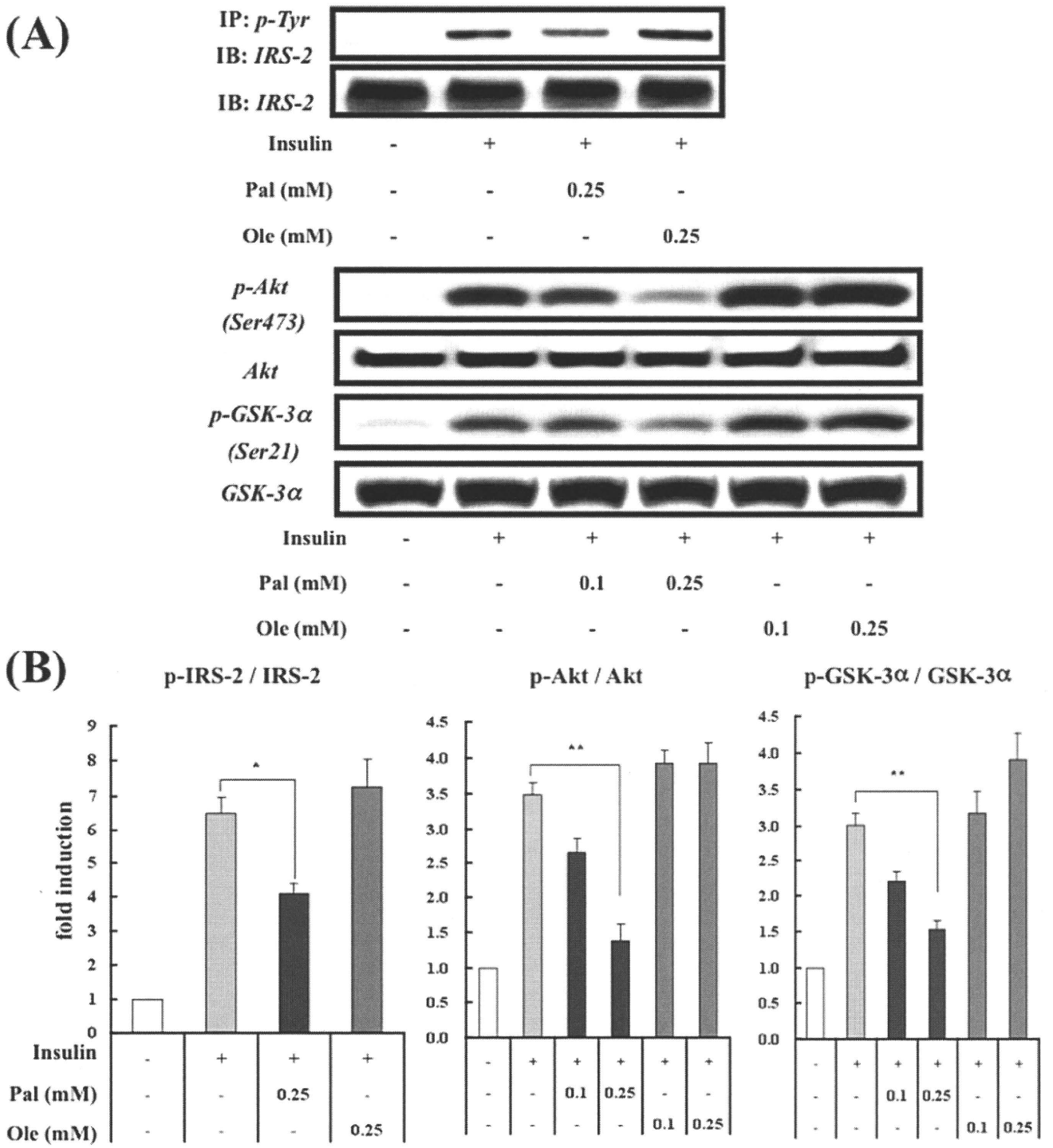

FIGURE 1. **Effects of palmitate and oleate on insulin-stimulated tyrosine phosphorylation of IRS-2 and serine phosphorylation of Akt and GSK-3 in H4IIEC3 hepatocytes.** *A*, H4IIEC3 cells were incubated in the presence or absence of palmitate (*Pal*) or oleate (*Ole*) for 16 h prior to stimulation with insulin (1 ng/ml, 15 min). Total cell lysates were resolved by SDS-PAGE, transferred to a PVDF membrane, and immunoblotted (*IB*) with the indicated antibodies. Total cell lysates were subjected to immunoprecipitation (*IP*) with phosphotyrosine antibody prior to SDS-PAGE to examine tyrosine phosphorylation of IRS-2. Detection was by enhanced chemiluminescence. Representative blots are shown. *B*, the values from densitometry of three (p-IRS-2), eight (p-Akt), or five (p-GSK-3α) independent experiments were normalized to the level of total IRS-2, Akt, or GSK-3α protein, respectively, and expressed as the mean -fold increase over control ± S.E. *, $p < 0.05$ *versus* insulin treatment alone. **, $p < 0.01$ *versus* insulin treatment alone.

EXPERIMENTAL PROCEDURES

Materials—The antibody against IRS-2 was purchased from Upstate Biotechnology, Inc. (Lake Placid, NY). Antibodies against phosphotyrosine, Akt, phospho-Akt (Ser^{473}), stress-activated protein kinase/JNK, phospho-stress-activated protein kinase/JNK (Thr^{183}/Tyr^{185}), and phospho-GSK (glycogen synthase kinase)-3 ($Ser^{21/9}$) were purchased from Cell Signaling Technology (Beverly, MA). Antibodies against GSK-3 and phospho-c-Jun were from Santa Cruz Biotechnology, Inc. (Santa Cruz, CA). Insulin from porcine pancreas, sodium

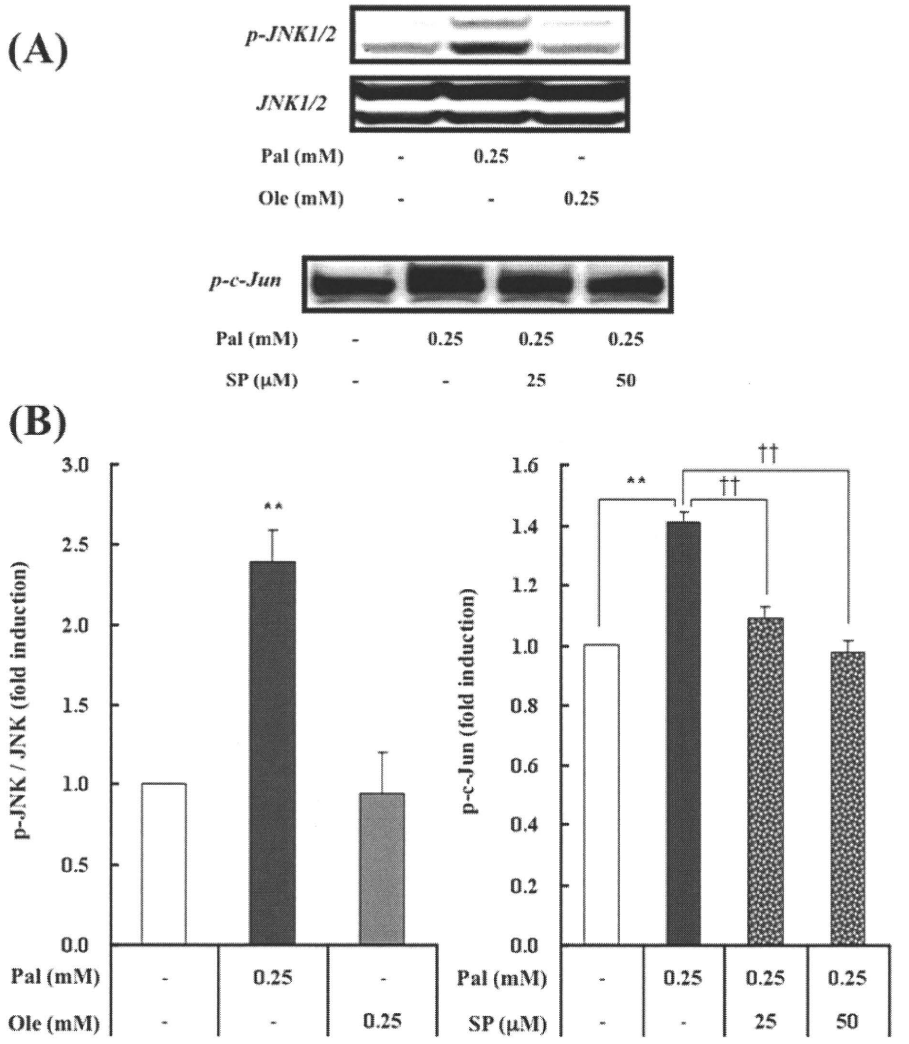

FIGURE 2. **Effects of palmitate and oleate on JNK activation in H4IIEC3 hepatocytes.** *A*, H4IIEC3 cells were incubated in the presence or absence of FFAs (palmitate (*Pal*) or oleate (*Ole*)) and the JNK inhibitor SP600125 (*SP*) for 16 h. Total cell lysates were resolved by SDS-PAGE, transferred to a PVDF membrane, and immunoblotted with the indicated antibodies. Detection was by enhanced chemiluminescence. Representative blots are shown. *B*, the values from densitometry of four (p-JNK) independent experiments were normalized to the level of total JNK (p-c-Jun was not normalized; $n = 4$) and expressed as the mean -fold increase over control ± S.E. **, $p < 0.01$ *versus* control. ††, $p < 0.01$ *versus* palmitate treatment.

palmitate, sodium oleate, myriocin, *N*-acetyl-L-cysteine, rotenone, thenoyltrifluoroacetone, cyanide *m*-chlorophenylhydrazone, oxypurinol, etomoxir, and tunicamycin was obtained from Sigma. SP600125 and apocynin were from Calbiochem. DL-α-tocopherol and 2′,7′-dichlorofluorescin diacetate (H_2DCFDA) were from Wako (Osaka, Japan).

Cell Culture and Fatty Acid Treatment—Studies were performed in the rat hepatoma cell line H4IIEC3, purchased from the American Type Culture Collection (Manassas, VA). Cells were cultured in Dulbecco's modified Eagle's medium (Invitrogen) supplemented with 10% fetal bovine serum (Invitrogen), penicillin (100 units/ml), and streptomycin (0.1 mg/ml; Invitrogen). The cells were cultured at 37 °C in a humidified atmosphere containing 5% CO_2, with medium changes three times a week. All studies were conducted using 80–90% confluent cells, which were treated with the indicated concentrations of FFAs in the presence of 2% FFA-free bovine serum albumin (Sigma).

Cell Harvest and Western Blot Analysis—H4IIEC3 hepatocytes, grown to 80–90% confluence in 6-well plates, were treated with the indicated reagents for 16 h in Dulbecco's modified Eagle's medium. After treatment, the cells were stimulated with insulin (1 ng/ml) for 15 min. Then the cells were washed with ice-cold phosphate-buffered saline and lysed in buffer containing 20 mM Tris-HCl (pH 7.5), 5 mM EDTA, 1% Nonidet P-40, 2 mM Na_3VO_4, 100 mM NaF, and a protease inhibitor mixture (Sigma). After sonication with a Bioruptor (Cosmo Bio, Tokyo, Japan), the lysates were centrifuged to remove insoluble materials. The supernatants (10 μg/lane) were separated by SDS-PAGE and transferred onto polyvinylidene difluoride membranes (Millipore, Billerica, MA). For detection of phosphotyrosine insulin receptor and phosphotyrosine IRS-2, the supernatants (400 μg of protein) were immunoprecipitated with a phosphotyrosine antibody and protein G beads for 2 h at 4 °C before SDS-PAGE. The membranes were blocked in a buffer containing 5% nonfat milk, 50 mM Tris (pH 7.6), 150 mM NaCl, and 0.1% Tween 20 (TBS-T) for 1 h at room temperature. They were then incubated with specific primary antibodies and subsequently with horseradish peroxidase-linked secondary antibodies. Signals were detected with a chemiluminescence detection system (ECL Plus Western blotting detection reagents; GE Healthcare). Densitometric analysis was conducted directly on the blotted membrane, using a CCD camera system (LAS-3000 Mini; Fujifilm, Tokyo, Japan) and Scion Image software.

Quantitative Real Time PCR—Total RNA was extracted from cultured H4IIEC3 hepatocytes using an RNeasy mini kit (Qiagen, Germantown, MD), according to the manufacturer's protocol. The cDNA was synthesized from total RNA (100 ng) using random hexamer primers, N_6, and a high capacity cDNA reverse transcription kit (Applied Biosystems, Foster City, CA). Quantitative real time PCR was performed with an ABI Prism 7900HT (Applied Biosystems). The set of specific primers and TaqMan probes in the present study was obtained from Applied Biosystems. The PCR conditions were one cycle at 50 °C for 2 min and 95 °C for 10 min, followed by 40 cycles at 95 °C for 15 s and 60 °C for 1 min.

Analysis of XBP-1 (X-box-binding Protein-1) mRNA Splicing—Total RNA was extracted from H4IIEC3 hepatocytes, and

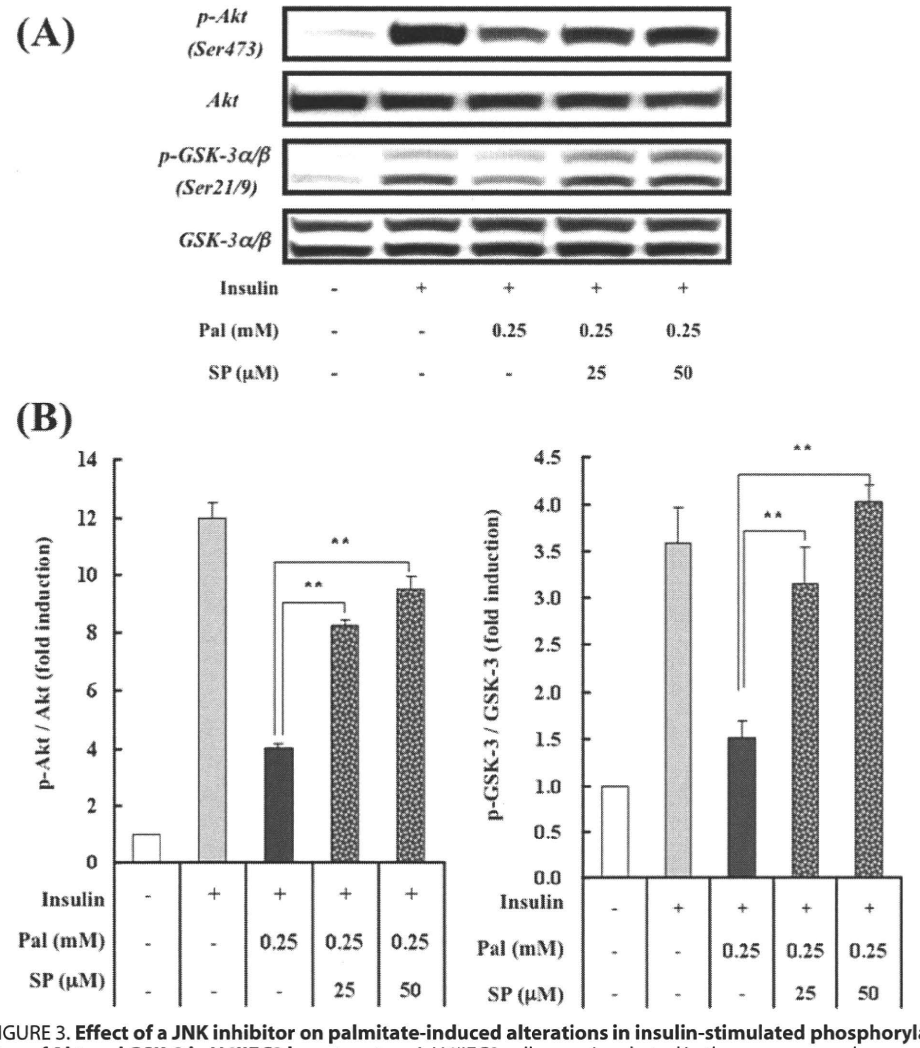

FIGURE 3. **Effect of a JNK inhibitor on palmitate-induced alterations in insulin-stimulated phosphorylation of Akt and GSK-3 in H4IIEC3 hepatocytes.** *A*, H4IIEC3 cells were incubated in the presence or absence of palmitate (*Pal*) and the JNK inhibitor SP600125 (*SP*) for 16 h prior to stimulation with insulin (1 ng/ml, 15 min). Total cell lysates were resolved by SDS-PAGE, transferred to a PVDF membrane, and immunoblotted with the indicated antibodies. Detection was enhanced by chemiluminescence. Representative blots are shown. *B*, the values from densitometry of four (p-Akt or p-GSK-3) independent experiments were normalized to the level of total Akt or GSK-3 protein, respectively, and expressed as the mean -fold increase over control ± S.E. **, $p <$ 0.01 *versus* palmitate treatment.

cDNA was synthesized as described above. The cDNA was amplified with a pair of primers (reverse 5′-CCA TGG GAA GAT GTT CTG GG-3′ and forward 5′-ACA CGC TTG GGG ATG AAT GC-3′) corresponding to the rat XBP-1 cDNA. The PCR conditions were initial denaturation at 94 °C for 3 min, followed by 30 cycles of amplification (94 °C for 30 s, 58 °C for 30 s, 72 °C for 30 s) and a final extension at 72 °C for 3 min. The PCR products were separated by 2.5% agarose gel electrophoresis.

Measurement of Intracellular ROS—The intracellular formation of ROS was detected using the fluorescent probe H_2DCFDA, according to a published method (13). Briefly, H4IIEC3 hepatocytes, grown to 70 – 80% confluence in 96-well plates, were treated with the indicated reagents in Dulbecco's modified Eagle's medium for 8 h. After treatment, the cells were washed with phosphate-buffered saline, loaded with 10 μM H_2DCFDA, and incubated for 30 min at 37 °C. The fluorescence was analyzed using a plate reader (Fluoroskan Ascent FL, ThermoLab Systems, Franklin, MA).

Measurement of Protein Carbonyls—The cellular concentration of proteins containing carbonyl groups (those that react with 2,4-dinitrophenylhydrazine to form the corresponding hydrazone) was determined spectrophotometrically using a protein carbonyl assay kit (Cayman Chemical, Ann Arbor, MI) according to the manufacturer's instructions and as described previously (14).

Statistical Analysis—All values are given as means ± S.E. Differences between two groups were assessed using unpaired, two-tailed *t* tests. Data involving more than two groups were assessed by one-way analysis of variance. All calculations were performed with SPSS (version 12.0 for Windows; SPSS, Chicago, IL).

RESULTS

Palmitate Inhibited Insulin Receptor-mediated Signaling—Two long chain fatty acids were chosen for the study: palmitate, a C16:0 saturated fatty acid, and oleate, a C18:1 monounsaturated fatty acid. To examine whether FFAs impaired insulin signal transduction in H4IIEC3 hepatocytes, we assessed the effect of FFAs on insulin-stimulated tyrosine phosphorylation of IRS-2 and serine phosphorylation of Akt and GSK-3α (Fig. 1). Incubation with 0.25 mM palmitate inhibited insulin-stimulated tyrosine phosphorylation of IRS-2 by 40% in H4IIEC3 cells. Downstream of IRS-2, insulin-stimulated serine phosphorylation of Akt and GSK-3α were also inhibited by 0.25 mM palmitate treatment, by 80 and 70%, respectively, indicating an insulin-resistant state. However, the protein levels of total IRS-2, Akt, and GSK-3 were unaffected by palmitate. Furthermore, we confirmed that palmitate, but not oleate, impaired insulin-stimulated Akt serine phosphorylation in the human hepatoma cell line HepG2 (supplemental Fig. 1).

JNK Activation by Palmitate Contributes to Palmitate-induced Insulin Resistance—JNK, a stress-activated protein kinase, has been reported to phosphorylate IRS-1 and -2 at serine residues (15, 16). Serine phosphorylation of IRSs impairs IRS tyrosine phosphorylation, leading to a reduction in insulin receptor-mediated signaling. Many studies have verified the role of JNK in fat-induced insulin resistance in several experimental systems (7, 17, 18). Thus, we next examined the effect of FFAs on JNK activation and its involvement in insulin signaling. Palmitate, but not oleate, dramatically increased phosphoryla-

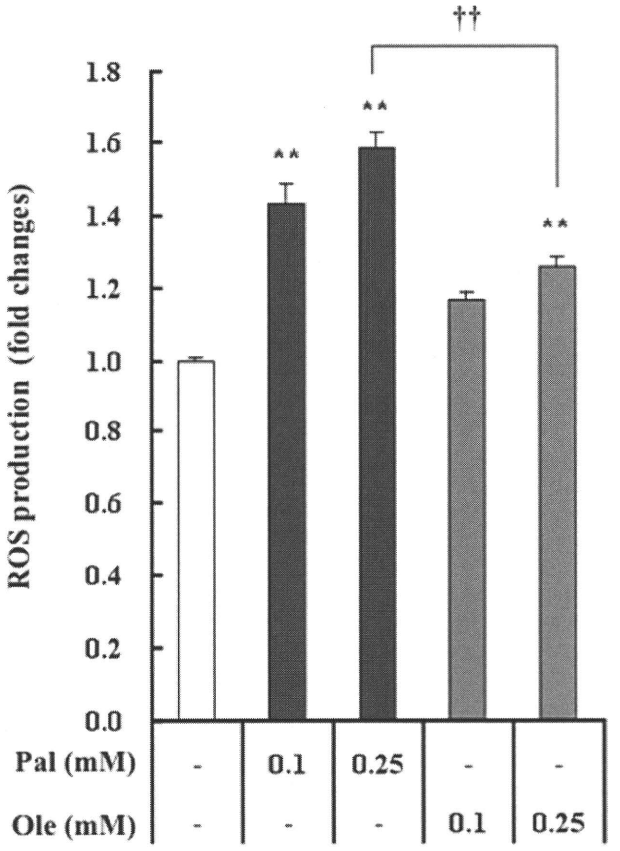

FIGURE 4. **Effect of palmitate on oxidative stress in H4IIEC3 hepatocytes.** H4IIEC3 cells were incubated in the presence or absence of palmitate (*Pal*) or oleate (*Ole*) for 8 h. Intracellular ROS production was quantified using the fluorescent probe H_2DCFDA. The values are expressed as mean -fold increase over control ± S.E. ($n = 4$). **, $p < 0.01$ *versus* control. ††, $p < 0.01$ *versus* 0.25 mM palmitate treatment.

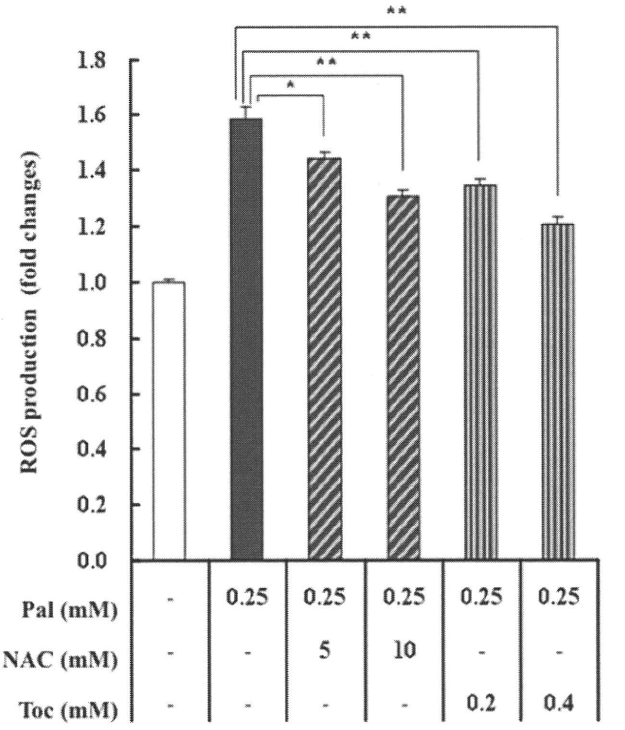

FIGURE 5. **Effects of antioxidants on palmitate-induced intracellular ROS production in H4IIEC3 hepatocytes.** H4IIEC3 cells were incubated in the presence or absence of palmitate (*Pal*) and antioxidants for 8 h. Intracellular ROS production was quantified using the fluorescent probe H_2DCFDA. The values are expressed as mean -fold increase over control ± S.E. ($n = 4$). *, $p < 0.05$ *versus* palmitate treatment alone. **, $p < 0.01$ *versus* palmitate treatment alone. *NAC*, *N*-acetyl-L-cysteine; *Toc*, α-tocopherol.

ted JNK and c-Jun (Fig. 2). A potent and selective inhibitor of JNK, SP600125 (19), reversed the palmitate-induced phosphorylation of c-Jun (Fig. 2), suggesting that palmitate activated JNK. To test whether palmitate-induced JNK activation mediated cellular insulin resistance, we inhibited the JNK pathway with SP600125. SP600125 dose-dependently improved insulin-stimulated serine phosphorylation of Akt and GSK-3 in H4IIEC3 hepatocytes exposed to palmitate (Fig. 3). These results suggest that JNK activation by palmitate contributed to palmitate-induced insulin resistance.

Pathways for SREBP-1c and ER Stress Are Not Involved in Palmitate-induced JNK Activation and Insulin Resistance in H4IIEC3 Hepatocytes—The SREBP-1c pathway has been reported to play a role in diet-induced insulin resistance *in vivo*. Ide *et al.* (6) found that high sucrose diet-induced hyperglycemia and hyperinsulinemia up-regulated hepatic expression of SREBP-1c, leading to down-regulation of IRS-2 at the transcriptional level. However, in the present study, palmitate dramatically down-regulated the expression of SREBP-1c in H4IIEC3 hepatocytes (supplemental Fig. 2). Consistent with this, the mRNA (supplemental Fig. 2) and protein (Fig. 1) levels of IRS-2 were unaffected by palmitate. Thus, palmitate itself did not appear to cause insulin resistance in hepatocytes via the SREBP-1c pathway.

ER stress is induced in insulin-resistant states, such as obesity and type 2 diabetes, and in turn, this stress has been shown to lead to the inhibition of insulin signaling, through overactivation of JNK (9). Since excessive FFAs have been shown to trigger ER stress in pancreatic β-cells (20), we examined whether palmitate caused ER stress in H4IIEC3 hepatocytes. ER stress induces the spliced form of XBP-1 (XBP-1s), which up-regulates the transcription of molecular chaperones, including GRP78 (78-kDa glucose-regulated/binding immunoglobulin protein) (21). Palmitate at 0.25 mM did not alter the expression level of GRP78 mRNA or the splicing pattern of XBP-1, unlike tunicamycin, an agent commonly used to induce ER stress (supplemental Fig. 3). Next, we compared the impact of palmitate and tunicamycin on insulin-stimulated signal transduction and JNK activation (supplemental Fig. 4). The inhibitory effect of tunicamycin on insulin-stimulated serine phosphorylation of Akt was mild and not significant compared with that of palmitate. Additionally, the increment in phosphorylated JNK by tunicamycin was lower and not significant compared with that of palmitate. These results suggest that ER stress played a minor role in palmitate-induced JNK activation and cellular insulin resistance in H4IIEC3 hepatocytes.

Palmitate Induces ROS Production—In addition to ER stress, increased cellular ROS levels are known to stimulate threonine phosphorylation of JNK (22). Indeed, ROS levels are increased in clinical conditions associated with insulin resistance, such as sepsis, burn injuries, obesity, and type 2 diabetes (23). Furthermore, FFAs have been reported to generate ROS in various

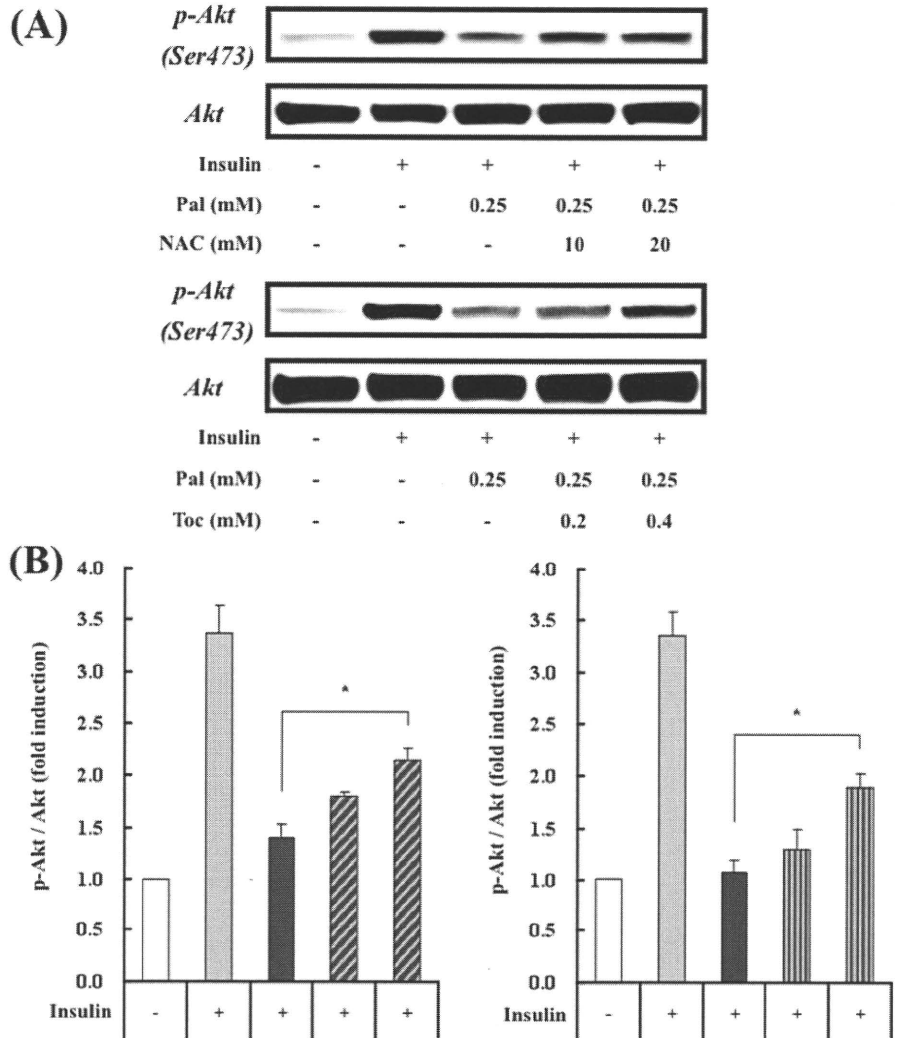

FIGURE 6. **Effects of antioxidants on palmitate-induced alterations in insulin-stimulated serine phosphorylation of Akt in H4IIEC3 hepatocytes.** *A*, H4IIEC3 cells were incubated in the presence or absence of palmitate (*Pal*) and antioxidants for 16 h prior to stimulation with insulin (1 ng/ml, 15 min). Total cell lysates were resolved by SDS-PAGE, transferred to a PVDF membrane, and immunoblotted with the indicated antibodies. Detection was by enhanced chemiluminescence. Representative blots are shown. *B*, the values from densitometry of four (NAC) or five (α-tocopherol) independent experiments were normalized to the level of total Akt protein and expressed as the mean -fold increase over control ± S.E. *, $p < 0.05$ *versus* palmitate treatment. *NAC*, *N*-acetyl-L-cysteine; *Toc*, α-tocopherol.

cells, such as pancreatic islet cells (24), cardiac myocytes (25), and adipocytes (23).

Thus, we hypothesized that palmitate increased intracellular ROS production and thereby activated JNK, leading to the impaired insulin signaling. To evaluate this, H4IIEC3 hepatocytes were incubated with H_2DCFDA, a fluorescent probe, to visualize intracellular ROS, with or without palmitate. H_2DCFDA-associated fluorescence was elevated by 58% after incubation with 0.25 mM palmitate for 8 h, and palmitate induced more ROS production than oleate (Fig. 4). Consistent with this, the amount of protein carbonyls, a marker of oxidative stress, significantly increased in palmitate-treated hepatocytes (4.6 ± 0.5 nmol/mg protein), compared with control cells (3.1 ± 0.4 nmol/mg protein). These results suggest that FFAs, especially palmitate, can cause ROS production and oxidative stress in H4IIEC3 hepatocytes.

Antioxidants Prevent Palmitate-induced Insulin Resistance—We next sought to test whether palmitate-induced ROS overproduction had a causal role in insulin resistance by assessing whether two antioxidant reagents, *N*-acetyl-L-cysteine (NAC) and α-tocopherol, could also act as insulin sensitizers. NAC and α-tocopherol dose-dependently suppressed palmitate-induced intracellular ROS production; NAC at 10 mM and α-tocopherol at 0.4 mM suppressed ROS production by 50 and 60%, respectively (Fig. 5). In parallel with decreased ROS levels, the antioxidants recovered the insulin-stimulated Akt phosphorylation impaired by palmitate; NAC at 10 mM and α-tocopherol at 0.4 mM recovered the phosphorylation by 40 and 35%, respectively (Fig. 6). Furthermore, these antioxidants suppressed palmitate-induced JNK phosphorylation; NAC at 10 mM and α-tocopherol at 0.4 mM suppressed it by 80 and 55%, respectively (Fig. 7). These results suggest that palmitate increased ROS levels in H4IIEC3 hepatocytes and thereby activated JNK, resulting in insulin resistance.

Palmitate Induces ROS Overproduction in Mitochondria—To define the source of ROS induced by palmitate in H4IIEC3 hepatocytes, we examined the cellular pathway involved in ROS production, including NADPH oxidase, xanthine oxidase, and mitochondria-mediated pathways. Palmitate-induced ROS production was markedly suppressed by rotenone, an inhibitor of mitochondrial respiratory chain complex I; thenoyltrifluoroacetone, an inhibitor of mitochondrial respiratory chain complex II; and carbonyl cyanide *m*-chlorophenylhydrazone, an uncoupler of oxidative phosphorylation (Fig. 8). In contrast, ROS production in palmitate-treated H4IIEC3 cells was not suppressed by apocynin, an inhibitor of NADPH oxidase, or oxypurinol, an inhibitor of xanthine oxidase. These results suggest that the mitochondrial respiratory chain is involved in palmitate-induced ROS overproduction in H4IIEC3 hepatocytes.

Palmitate Increases ROS through the Mitochondrial Fatty Acid β-Oxidation Respiratory Chain—FFAs are metabolized in the mitochondrial fatty acid β-oxidation pathway, which sup-

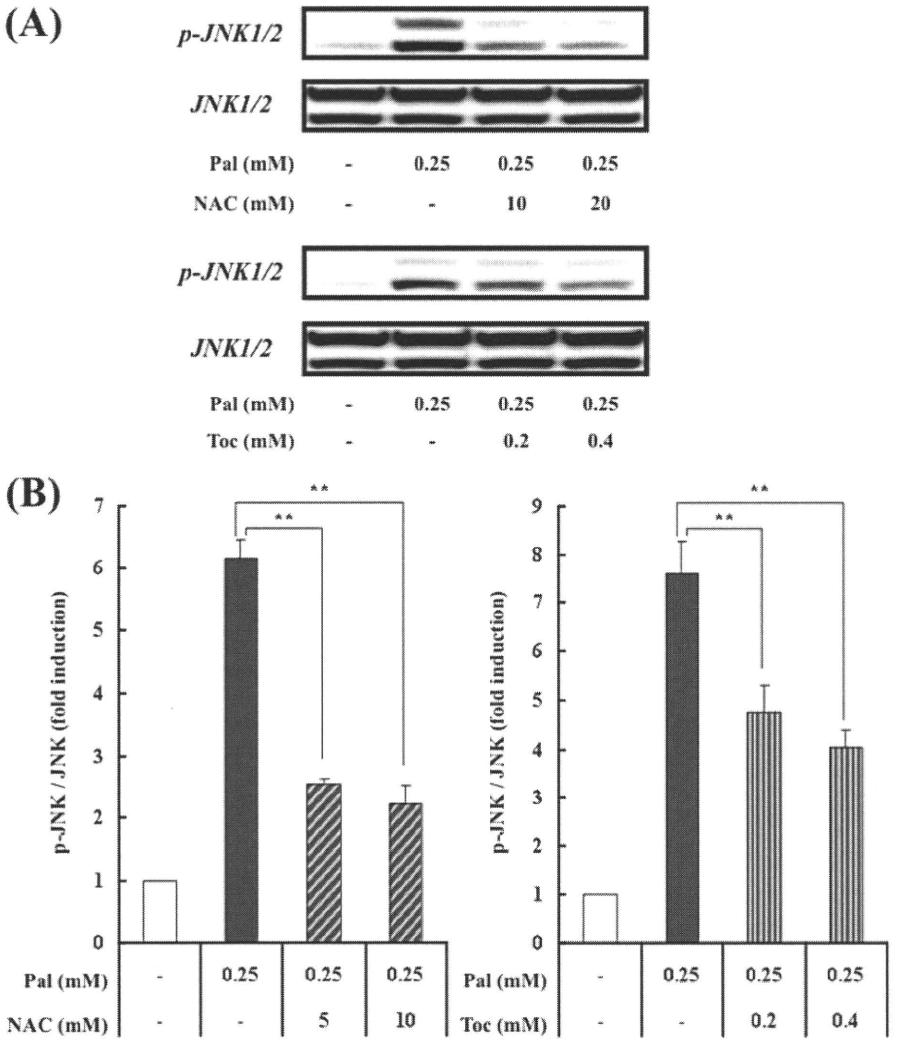

FIGURE 7. **Effects of antioxidants on palmitate-induced JNK activation in H4IIEC3 hepatocytes.** *A*, H4IIEC3 cells were incubated in the presence or absence of palmitate (*Pal*) and antioxidants for 16 h. Total cell lysates were resolved by SDS-PAGE, transferred to a PVDF membrane, and immunoblotted with the indicated antibodies. Detection was by enhanced chemiluminescence. Representative blots are shown. *B*, the values from densitometry of four (NAC or α-tocopherol) independent experiments were normalized to the level of total JNK protein and expressed as the mean -fold increase over control ± S.E. **, $p < 0.01$ *versus* palmitate treatment alone. *Toc*, α-tocopherol.

plies the mitochondrial respiratory chain with electrons. Large amounts of electrons entering the respiratory chain may cause abnormal reduction of oxygen, leading to ROS production. Thus, we next examined whether palmitate-induced ROS production was dependent on mitochondrial fatty acid β-oxidation. CPT-1a (carnitine palmitoyltransferase-1a) is the rate-limiting enzyme in mitochondrial fatty acid β-oxidation. As expected, etomoxir, a CPT-1 inhibitor, decreased palmitate-induced ROS production, by 80% (Fig. 9*A*). Furthermore, palmitate, but not oleate, significantly increased expression of the *CPT-1a* gene (Fig. 9*B*). This up-regulation may contribute to palmitate-induced ROS overproduction, because the accelerated β-oxidation should cause excessive electron flux in the respiratory chain.

DISCUSSION

In the present study, we investigated the direct action of fatty acids on insulin signaling in hepatocytes. The saturated fatty acid palmitate, but not the unsaturated fatty acid oleate, impaired insulin-induced tyrosine phosphorylation of IRS-2, serine phosphorylation of Akt, and serine phosphorylation of GSK-3α, all of which are indicative of insulin resistance in cultured H4IIEC3 hepatocytes (Fig. 10). Unlike *in vivo* findings (6), the expression of the *SREBP-1c* gene was down-regulated by adding palmitate to cultured H4IIEC3 hepatocytes, which is likely a result of a negative feedback loop for fatty acid synthesis, and IRS-2 protein levels were unaffected. FFA-induced insulin resistance has been reported in other insulin-sensitive cells, such as adipocytes (18) and skeletal muscle cells (26). These studies, together with the present results, suggest that FFA inhibits insulin signaling at the level of tyrosine phosphorylation of IRSs, regardless of cell type. Similar to the findings in 3T3-L1 adipocytes (18) and primary mouse hepatocytes and pancreatic β-cells (16), the activation of JNK, a known suppressor of the tyrosine phosphorylation of IRSs, was involved in FFA-induced tyrosine phosphorylation of IRS-2 in cultured H4IIEC3 hepatocytes. Because a JNK inhibitor, SP600125, largely restored palmitate-induced impairment of the insulin signaling pathway, JNK activation seems to play a major role in the development of palmitate-induced insulin resistance in H4IIEC3 hepatocytes. Our results support *in vivo* findings that JNK is activated in the liver of an animal model of obesity and diabetes in which FFA influx into the liver is elevated (9, 27). The overexpression of JNK in mouse liver resulted in hepatic insulin resistance at the level of IRS tyrosine phosphorylation, and the overexpression of a dominant negative mutant of JNK in the liver accelerated hepatic insulin signaling (17).

Given that JNK is activated by many types of cellular stresses (28), we next searched for a link between palmitate treatment and JNK activation in H4IIEC3 hepatocytes. ER stress was unlikely to mediate palmitate-induced insulin resistance in H4IIEC3 hepatocytes, because palmitate caused insulin resistance independent of ER stress, whereas tunicamycin caused ER stress without affecting insulin action. Instead, we found that palmitate-induced ROS generation mediated insulin resistance. ROS are one of many factors suggested to have a possible role in insulin resistance (29, 30). ROS include reactive products, such as superoxide anion, hydrogen peroxide, and

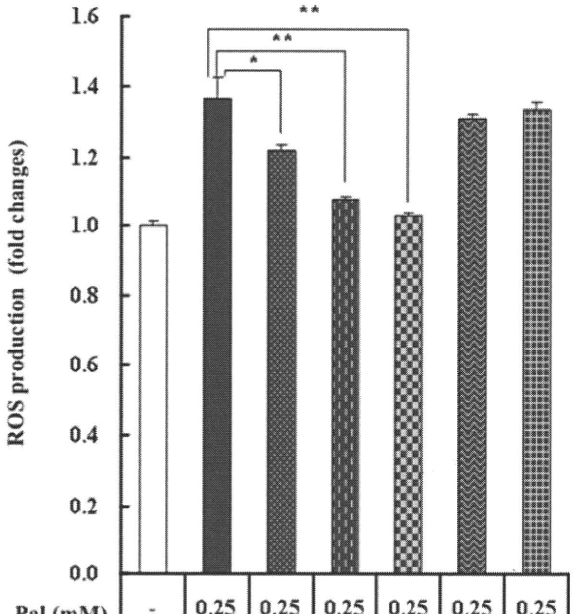

FIGURE 8. **Effects of ROS-producing pathway inhibitors on palmitate-induced ROS production in H4IIEC3 hepatocytes.** H4IIEC3 cells were incubated in the presence or absence of palmitate (*Pal*) and each ROS-producing pathway inhibitor for 8 h. Intracellular ROS production was quantified using the fluorescent probe H_2DCFDA. The values are expressed as mean -fold increase over control ± S.E. ($n = 4$). *, $p < 0.05$ *versus* palmitate treatment alone. **, $p < 0.01$ *versus* palmitate treatment alone. *Rot*, rotenone; *Apo*, apocynin; *Oxy*, oxypurinol; *TTFA*, thenoyltrifluoroacetone; *CCCP*, carbonyl cyanide *m*-chlorophenylhydrazone.

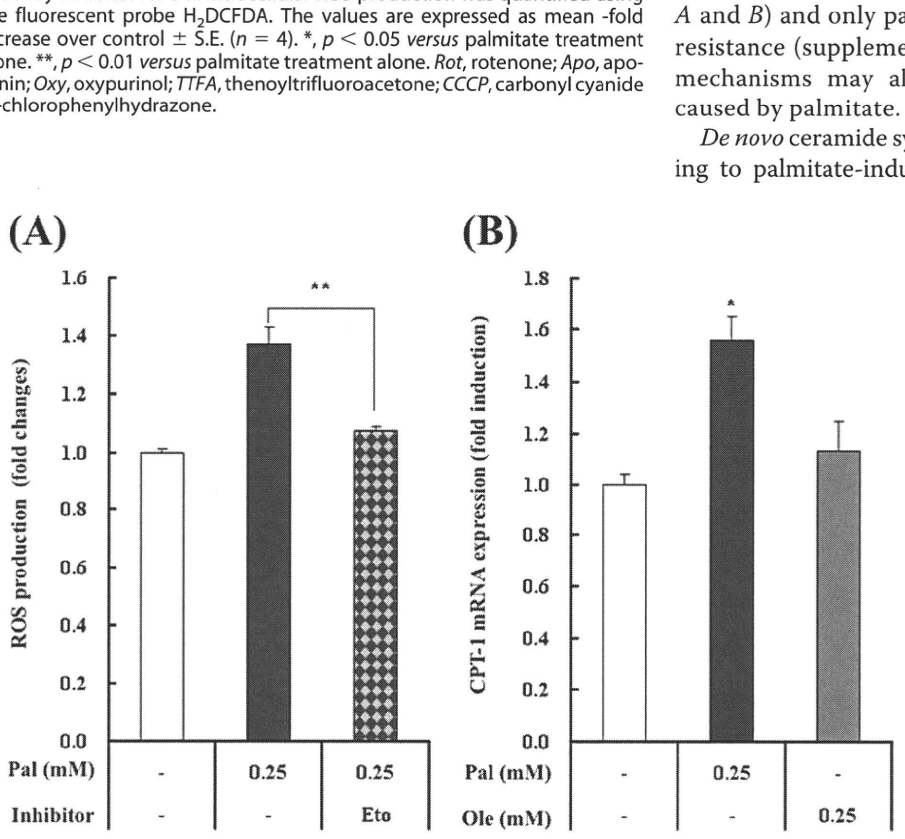

FIGURE 9. **Involvement of mitochondrial fatty acid oxidation in palmitate-induced ROS production.** *A*, H4IIEC3 cells were incubated in the presence or absence of palmitate (*Pal*) and the CPT-1 inhibitor etomoxir (*Eto*) for 8 h. Intracellular ROS production was quantified using the fluorescent probe H_2DCFDA. The values are expressed as mean -fold increase over control ± S.E. ($n = 4$). *B*, H4IIEC3 cells were incubated in the presence or absence of palmitate (*Pal*) or oleate (*Ole*) for 16 h. Total RNA was extracted and subjected to reverse transcription. Using the cDNA as a template, the amounts of CPT-1 mRNA were detected by real time PCR. The values were normalized to the level of 18 S ribosomal RNA and expressed as mean -fold increase over control ± S.E. ($n = 3$). *, $p < 0.05$ *versus* control. **, $p < 0.01$ *versus* palmitate treatment alone.

hydroxyl radical, which are formed as by-products of mitochondrial oxidative phosphorylation (OXPHOS). Thus, as a rule, increased mitochondrial OXPHOS flux leads to increased formation of ROS (31, 32). ROS can also be produced during β-oxidation of fatty acids, especially as a by-product of peroxisomal acyl-CoA oxidase activity (32). Additionally, ROS can be produced by dedicated enzymes, such as NADPH oxidase (33), present in phagocytic cells, where ROS are an important part of cellular defense mechanisms. Using specific inhibitors of subcellular ROS, we identified mitochondrial OXPHOS as an important source of palmitate-induced ROS generation in H4IIEC3 hepatocytes. FFAs supply mitochondrial OXPHOS with electrons through mitochondrial fatty acid β-oxidation. A final metabolite of fatty acids, acetyl-CoA, is metabolized in the trichloroacetic acid cycle. In the processes of fatty acid β-oxidation and the trichloroacetic acid cycle, NADH and $FADH_2$ are generated and could supply excessive electrons for OXPHOS.

NAC, a scavenger of ROS, dose-dependently restored glutathione in palmitate-treated cells (supplemental Fig. 5). However, glutathione restoration by NAC was unable to completely rescue palmitate-induced insulin resistance. Furthermore, the combination of NAC and α-tocopherol did not completely reverse JNK activation (supplemental Fig. 6, *A* and *B*) and only partly rescued palmitate-induced insulin resistance (supplemental Fig. 7, *A* and *B*). Therefore, other mechanisms may also be involved in insulin resistance caused by palmitate.

De novo ceramide synthesis is a potential pathway contributing to palmitate-induced JNK activation. Ceramide derived from saturated fatty acids has been reported to activate JNK and inhibit insulin-induced Akt phosphorylation in myocytes (34–36). In our investigation, palmitate increased the intracellular content of ceramide in H4IIEC3 hepatocytes (supplemental Fig. 8). Unfortunately, even at the maximum myriosin concentration, the intracellular accumulation of ceramide was not blocked by myriosin, a potent inhibitor of serine palmitoyltransferase at the first step in ceramide biosynthesis (supplemental Fig. 8). Furthermore, ceramide accumulation was not blocked when myriosin was used in combination with fumonisin B1, an inhibitor of ceramide synthase (data not shown). Therefore, we cannot rule out the possibility that intracellular ceramide contributes to palmitate-induced insulin resistance in H4IIEC3 hepatocytes. Further studies are required to assess the role of the

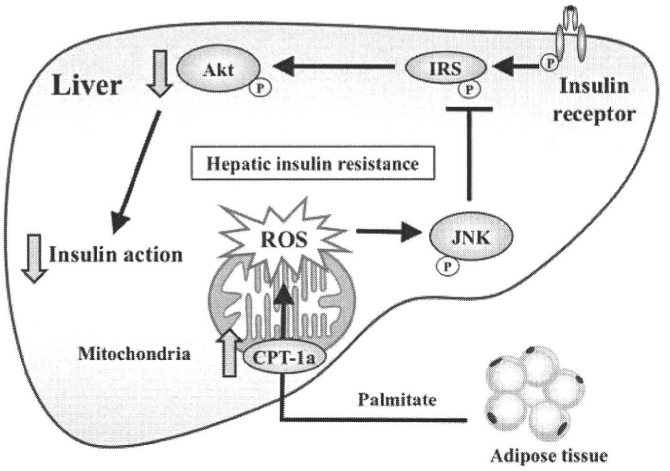

FIGURE 10. **Proposed model for palmitate-induced hepatic insulin resistance.**

ceramide pathway in palmitate-induced insulin resistance in hepatocytes.

In the present study, etomoxir, an inhibitor of CPT-1, decreased palmitate-induced intracellular ROS production. Additionally, palmitate, but not oleate, significantly increased the expression of the *CPT-1a* gene, which may account for the observed differences in insulin action between palmitate and oleate.

Recently, it was reported that fatty acid composition may be a determinant in insulin sensitivity (37, 38). In this regard, we investigated the effect of oleate on insulin signaling in palmitate-treated hepatocytes. Surprisingly, oleate dose-dependently reversed palmitate-induced ROS generation and JNK phosphorylation and rescued palmitate-induced phosphorylation of Akt.[3] Further investigations aimed at elucidating the molecular basis underlying the differential roles and interactions of FFAs are required.

In conclusion, this study identified mitochondrial ROS generation as a critical factor in palmitate-induced hepatic insulin resistance. Palmitate may induce CPT-1 expression, accelerate metabolism, supply excess electrons for mitochondrial OXPHOS, and generate ROS. ROS then desensitize the insulin signaling pathway by activating JNK, impairing tyrosine phosphorylation of IRS-2, and causing hepatic insulin resistance (Fig. 10). The results suggest that an initial event in high fat/sucrose diet-induced or obesity-induced insulin resistance in the liver is mitochondrial ROS generation, which could potentially be a therapeutic target. In addition to previously suggested JNK inhibitors or antioxidants, mitochondrial uncouplers, such as cyanide *m*-chlorophenylhydrazone, may provide a candidate therapeutic strategy for this pathway by preventing ROS generation.

Acknowledgments—We thank Drs. Isao Usui and Hajime Ishihara and Prof. Toshiyasu Sasaoka (Toyama University) for supplying technical expertise on Western blot analysis of phosphoproteins.

[3] H. Takayama and T. Takamura, unpublished data.

REFERENCES

1. Saltiel, A. R., and Kahn, C. R. (2001) *Nature* **414,** 799–806
2. Ota, T., Takamura, T., Kurita, S., Matsuzawa, N., Kita, Y., Uno, M., Akahori, H., Misu, H., Sakurai, M., Zen, Y., Nakanuma, Y., and Kaneko, S. (2007) *Gastroenterology* **132,** 282–293
3. Matsuzawa, N., Takamura, T., Kurita, S., Misu, H., Ota, T., Ando, H., Yokoyama, M., Honda, M., Zen, Y., Nakanuma, Y., Miyamoto, K., and Kaneko, S. (2007) *Hepatology* **46,** 1392–1403
4. Sakurai, M., Takamura, T., Ota, T., Ando, H., Akahori, H., Kaji, K., Sasaki, M., Nakanuma, Y., Miura, K., and Kaneko, S. (2007) *J. Gastroenterol.* **42,** 312–317
5. Boden, G. (1997) *Diabetes* **46,** 3–10
6. Ide, T., Shimano, H., Yahagi, N., Matsuzaka, T., Nakakuki, M., Yamamoto, T., Nakagawa, Y., Takahashi, A., Suzuki, H., Sone, H., Toyoshima, H., Fukamizu, A., and Yamada, N. (2004) *Nat. Cell Biol.* **6,** 351–357
7. Hirosumi, J., Tuncman, G., Chang, L., Gorgun, C. Z., Uysal, K. T., Maeda, K., Karin, M., and Hotamisligil, G. S. (2002) *Nature* **420,** 333–336
8. Boden, G., She, P., Mozzoli, M., Cheung, P., Gumireddy, K., Reddy, P., Xiang, X., Luo, Z., and Ruderman, N. (2005) *Diabetes* **54,** 3458–3465
9. Ozcan, U., Cao, Q., Yilmaz, E., Lee, A. H., Iwakoshi, N. N., Ozdelen, E., Tuncman, G., Gorgun, C., Glimcher, L. H., and Hotamisligil, G. S. (2004) *Science* **306,** 457–461
10. Kim, J. K., Fillmore, J. J., Chen, Y., Yu, C., Moore, I. K., Pypaert, M., Lutz, E. P., Kako, Y., Velez-Carrasco, W., Goldberg, I. J., Breslow, J. L., and Shulman, G. I. (2001) *Proc. Natl. Acad. Sci. U. S. A.* **98,** 7522–7527
11. Turinsky, J., O'Sullivan, D. M., and Bayly, B. P. (1990) *J. Biol. Chem.* **265,** 16880–16885
12. Du, K., Herzig, S., Kulkarni, R. N., and Montminy, M. (2003) *Science* **300,** 1574–1577
13. Nishikawa, T., Edelstein, D., Du, X. L., Yamagishi, S., Matsumura, T., Kaneda, Y., Yorek, M. A., Beebe, D., Oates, P. J., Hammes, H. P., Giardino, I., and Brownlee, M. (2000) *Nature* **404,** 787–790
14. Matsuzawa-Nagata, N., Takamura, T., Ando, H., Nakamura, S., Kurita, S., Misu, H., Ota, T., Yokoyama, M., Honda, M., Miyamoto, K., and Kaneko, S. (2008) *Metabolism* **57,** 1071–1077
15. Aguirre, V., Uchida, T., Yenush, L., Davis, R., and White, M. F. (2000) *J. Biol. Chem.* **275,** 9047–9054
16. Solinas, G., Naugler, W., Galimi, F., Lee, M. S., and Karin, M. (2006) *Proc. Natl. Acad. Sci. U. S. A.* **103,** 16454–16459
17. Nakatani, Y., Kaneto, H., Kawamori, D., Hatazaki, M., Miyatsuka, T., Matsuoka, T. A., Kajimoto, Y., Matsuhisa, M., Yamasaki, Y., and Hori, M. (2004) *J. Biol. Chem.* **279,** 45803–45809
18. Nguyen, M. T., Satoh, H., Favelyukis, S., Babendure, J. L., Imamura, T., Sbodio, J. I., Zalevsky, J., Dahiyat, B. I., Chi, N. W., and Olefsky, J. M. (2005) *J. Biol. Chem.* **280,** 35361–35371
19. Bennett, B. L., Sasaki, D. T., Murray, B. W., O'Leary, E. C., Sakata, S. T., Xu, W., Leisten, J. C., Motiwala, A., Pierce, S., Satoh, Y., Bhagwat, S. S., Manning, A. M., and Anderson, D. W. (2001) *Proc. Natl. Acad. Sci. U. S. A.* **98,** 13681–13686
20. Karaskov, E., Scott, C., Zhang, L., Teodoro, T., Ravazzola, M., and Volchuk, A. (2006) *Endocrinology* **147,** 3398–3407
21. Harding, H. P., Calfon, M., Urano, F., Novoa, I., and Ron, D. (2002) *Annu. Rev. Cell Dev. Biol.* **18,** 575–599
22. Kaneto, H., Kawamori, D., Nakatani, Y., Gorogawa, S., and Matsuoka, T. A. (2004) *Drug News Perspect.* **17,** 447–453
23. Furukawa, S., Fujita, T., Shimabukuro, M., Iwaki, M., Yamada, Y., Nakajima, Y., Nakayama, O., Makishima, M., Matsuda, M., and Shimomura, I. (2004) *J. Clin. Invest.* **114,** 1752–1761
24. Carlsson, C., Borg, L. A., and Welsh, N. (1999) *Endocrinology* **140,** 3422–3428
25. Miller, T. A., LeBrasseur, N. K., Cote, G. M., Trucillo, M. P., Pimentel, D. R., Ido, Y., Ruderman, N. B., and Sawyer, D. B. (2005) *Biochem. Biophys. Res. Commun.* **336,** 309–315
26. Chavez, J. A., and Summers, S. A. (2003) *Arch. Biochem. Biophys.* **419,** 101–109
27. Nakatani, Y., Kaneto, H., Kawamori, D., Yoshiuchi, K., Hatazaki, M., Mat-

suoka, T. A., Ozawa, K., Ogawa, S., Hori, M., Yamasaki, Y., and Matsuhisa, M. (2005) *J. Biol. Chem.* **280,** 847–851
28. Davis, R. J. (2000) *Cell* **103,** 239–252
29. Evans, J. L., Goldfine, I. D., Maddux, B. A., and Grodsky, G. M. (2002) *Endocr. Rev.* **23,** 599–622
30. Houstis, N., Rosen, E. D., and Lander, E. S. (2006) *Nature* **440,** 944–948
31. Brownlee, M. (2001) *Nature* **414,** 813–820
32. Osmundsen, H., Bremer, J., and Pedersen, J. I. (1991) *Biochim. Biophys. Acta* **1085,** 141–158
33. De Minicis, S., Bataller, R., and Brenner, D. A. (2006) *Gastroenterology* **131,** 272–275
34. Chavez, J. A., Knotts, T. A., Wang, L. P., Li, G., Dobrowsky, R. T., Florant, G. L., and Summers, S. A. (2003) *J. Biol. Chem.* **278,** 10297–10303
35. Powell, D. J., Turban, S., Gray, A., Hajduch, E., and Hundal, H. S. (2004) *Biochem. J.* **382,** 619–629
36. Schmitz-Peiffer, C., Craig, D. L., and Biden, T. J. (1999) *J. Biol. Chem.* **274,** 24202–24210
37. Bruce, C. R., and Febbraio, M. A. (2007) *Nat. Med.* **13,** 1137–1138
38. Cao, H., Gerhold, K., Mayers, J. R., Wiest, M. M., Watkins, S. M., and Hotamisligil, G. S. (2008) *Cell* **134,** 933–944

Clinical and Experimental Hypertension, 31:201–207, 2009

ISSN: 1064-1963 print / 1525-6006 online
DOI: 10.1080/10641960902822450

informa
healthcare

Clock Gene Expression in the Liver and Adipose Tissues of Non-Obese Type 2 Diabetic Goto-Kakizaki Rats

HITOSHI ANDO,[1,2] KENTAROU USHIJIMA,[1]
HAYATO YANAGIHARA,[1] YOHEI HAYASHI,[1]
TOSHINARI TAKAMURA,[2] SHUICHI KANEKO,[2]
AND AKIO FUJIMURA[1]

[1]Division of Clinical Pharmacology, Department of Pharmacology, School of Medicine, Jichi Medical University, Tochigi, Japan
[2]Department of Disease Control and Homeostasis, Kanazawa University, Graduate School of Medical Science, Ishikawa, Japan

Recent studies have revealed a close relationship between the pathophysiology of metabolic syndrome, which is characterized by obesity and hyperglycemia, and the functioning of internal molecular clocks. In this study, we show that the rhythmic mRNA expression of clock genes (Clock, Bmal1, Cry1, and Dbp) is not attenuated in the liver and visceral adipose tissues of Goto-Kakizaki rats, a model of nonobese, type 2 diabetes, as compared to control Wistar rats. Our results suggest that molecular clock impairment in peripheral tissues of obese diabetic animals may be either caused by obesity-related factor(s), but not hyperglycemia, or be a cause, but not a consequence, of hyperglycemia.

Keywords circadian rhythm, clock gene, type 2 diabetes, metabolic syndrome, liver

Introduction

Various physiological and behavioral processes exhibit circadian (i.e., 24 h) rhythmicity, which in turn may play a pivotal role in maintaining functional homeostasis. Recent studies have revealed that these endogenous rhythms are generated at the cellular level by circadian core oscillators, composed of transcriptional/translational feedback loops involving a set of clock genes (1,2). In mammals, rhythmic transcriptional enhancement by two basic helix–loop–helix Per–Arnt–Sim domain-containing transcription factors, that is, CLOCK and brain and muscle Arnt-like protein 1 (BMAL1), provides the basic drive

Submitted August 20, 2007; revised December 19, 2007; accepted February 4, 2008.
Address correspondence to Akio Fujimura, MD, PhD, Department of Pharmacology, School of Medicine, Jichi Medical University, 3311-1 Yakushiji, Shimotsuke, Tochigi 329-0498, Japan; E-mail: akiofuji@jichi.ac.jp

for the intracellular clock system. Specifically, the CLOCK-BMAL1 heterodimer activates the transcription of various clock-controlled genes (3,4). Given that some clock-controlled genes, including the albumin D-site binding protein (Dbp), also serve as transcription factors, the expression of numerous genes may be tied to the functions of the molecular clock (1,2). In parallel, the heterodimer activates the transcription of several clock genes, including Period (Per) and Cryptochorome (Cry) (5–7). The resultant PER and CRY proteins translocate back into the nucleus and inhibit the activity of CLOCK-BMAL1, thus forming the negative feedback loop (1,2).

The molecular clock system resides not only in the hypothalamic suprachiasmatic nucleus (SCN), which is recognized as the central mammalian clock, but also in various peripheral tissues (8–11). The SCN is not essential for driving peripheral oscillations but acts to synchronize peripheral oscillators (10). Therefore, local molecular clocks may directly control the physiological rhythmicity of peripheral tissues.

Recently, type 2 diabetes mellitus has reached epidemic proportions (12). Pancreatic β-cell dysfunction and insulin resistance are key elements in the pathogenesis of type 2 diabetes and both contribute to the presence of hyperglycemia in this disease. In particular, insulin resistance is strongly associated with obesity, and several mechanisms mediating this interaction have been identified (12). For example, various humoral factors, so-called adipocytokines, which originate in adipose tissue, have been shown to modulate insulin action and may be involved in the development of various diseases including type 2 diabetes, hypertension, dyslipidemia, and cardiovascular disease (11,12). Interestingly, it has been demonstrated that clock mutant mice have an attenuated 24 h feeding rhythm, are hyperphagic and obese, and develop metabolic syndrome, including hyperglycemia and hyperlipidemia (13). In addition, BMAL1 and the clock gene Rev-erbα are known to be involved in the regulation of adipocyte differentiation (14,15). Impaired adipocyte differentiation, as well as increased adipocyte hypertrophy, plays major roles in the development of metabolic syndrome (16). Furthermore, previous studies have revealed that the rhythmic expression of clock genes is attenuated in the visceral adipose tissue and liver of genetically obese, diabetic mice (KK-A^y, ob/ob, and db/db mice) (11,17). Thus, a close relationship may exist between molecular clock functioning and the pathophysiology of obesity and/or type 2 diabetes. At this time, however, it remains to be elucidated whether type 2 diabetes, without obesity, is also associated with impaired molecular clock function. To address this issue, we investigated the rhythmic mRNA expression of clock genes in the visceral adipose tissue and liver of Goto-Kakizaki (GK) rats, a model of nonobese type 2 diabetes (18,19).

Materials and Methods

Rats

Eight-week-old male GK/Jcl and Wistar rats were obtained from CLEA Japan (Tokyo, Japan). All rats were maintained under specific pathogen-free conditions, controlled temperature, controlled humidity, and a 12-h light (07:00–19:00 h)/12-h dark (19:00–07:00 h) cycle. Rats were provided with a standard laboratory diet (CE-2, CLEA, Japan) and water *ad libitum*. After 2 weeks, animals were killed to obtain blood, liver, and epididymal fat samples at the following zeitgeber times (ZT): 0, 6, 12, and 18, where ZT 0 is defined as lights on and ZT 12 as lights off. All animal procedures were performed in accordance with the guidelines for animal research at Jichi Medical University, Japan.

Measuring Circulating Glucose and Insulin Concentrations

Blood glucose concentrations were measured using a Glutest Ace R diagnostic system (Sanwa Kagaku Kenkyusyo, Nagoya, Japan). The radioimmunoassay for serum insulin was performed using a commercial kit purchased from Linco Research (St. Charles, MO). The intra- and inter-assay coefficients of variation were less than 10%.

RNA Extraction and Real-Time Quantitative PCR

Isolation of total RNA was achieved using the RNeasy Mini Kit or the RNeasy Lipid Tissue Mini Kit, according to the manufacturer's instructions (Qiagen, Valencia, CA). Reverse transcription was performed with 1.2 μg of total RNA, random hexamer primers, and RevertAid M-MuLV reverse transcriptase (Fermentas, Hanover, MD). Gene expression was analyzed by real-time quantitative polymerase chain reaction (PCR) using the ABI Prism 7700 sequence detection system (Applied Biosystems, Foster City, CA), as previously described (11,20). All specific sets of primers and TaqMan probes were obtained from Applied Biosystems (TaqMan Gene Expression Assays and TaqMan Rodent GAPDH Control Reagents). To control for variation in the amount of DNA available for PCR in the different samples, gene expression levels of the target sequence were normalized in relation to the expression of an endogenous control, glyceraldehyde-3-phosphate dehydrogenase (GAPDH). Data were analyzed using the comparative threshold cycle method.

Statistical Analysis

Data were analyzed using either a Kruskal–Wallis test or a Mann–Whitney *U*-test. Values are presented as the means ± SE, and p values of less than 0.05 were considered significant. All calculations were performed using SPSS version 12.0.2J for Windows (SPSS Japan Inc., Tokyo, Japan).

Results

At 10 weeks of age, GK rats were lean and mildly hyperglycemic compared to control Wistar rats (Figure 1). Although hyperglycemia was present, serum insulin concentrations were not elevated as expected, suggesting that glucose-stimulated insulin secretion is

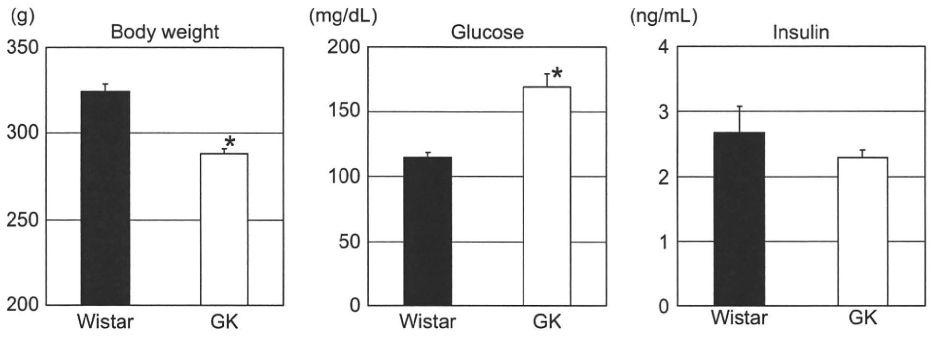

Figure 1. Biological characteristics of Wistar and GK rats at 10 weeks of age. Data are expressed as the means + SE of 16 rats in each group. *$P < 0.01$ vs. Wistar rats.

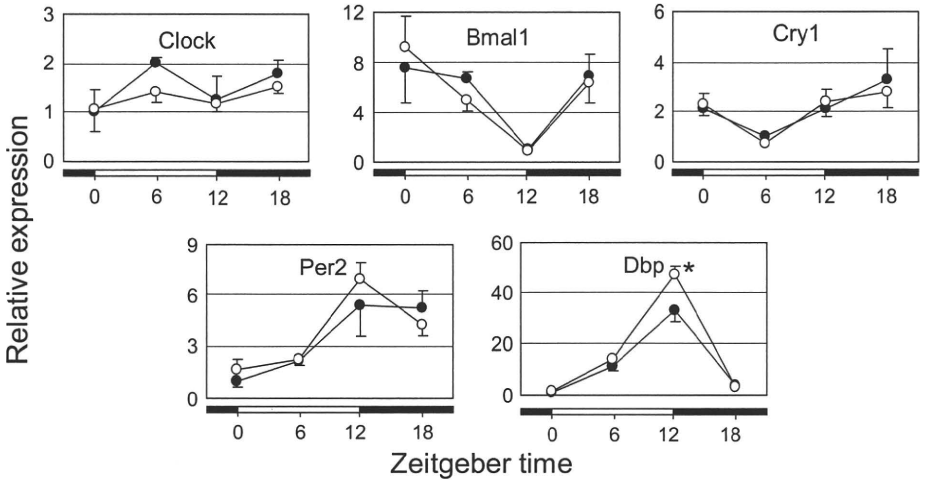

Figure 2. Daily mRNA expression profiles of clock genes in the visceral adipose tissues of Wistar (●—●) and GK (○—○) rats. Data are reported as the means and SE of four rats at each time point and are expressed as relative values (compared to the lowest values in Wistar rats) for each gene. $*P < 0.05$ vs. Wistar rats.

impaired in this strain. Thus, GK rats spontaneously developed glucose intolerance without obesity.

In the visceral adipose tissues of both Wistar and GK rats, mRNA expression of Bmal1, Per2, and Dbp showed significant 24-h rhythms (Figure 2; $\chi^2 = 8.5–14.1$, each $P < 0.05$, Kruskal–Wallis test). In a manner consistent with previous studies in mice (11), transcriptional levels of Per2 and Dbp peaked at ZT 12, whereas Bmal1 mRNA dropped to trough levels at that time. Conversely, rhythmic expression of Clock was not detected in either Wistar or GK rats (Figure 2). In contrast to obese, type 2 diabetic KK-A^y mice (11), peak levels of the clock genes Bmal1, Cry1, and Per2 were not diminished in GK rats. Instead, the rhythmic expression of Dbp, a marker of molecular clock function, appeared to be enhanced in GK rats. These results suggest that hyperglycemia without obesity does not impair the molecular clock system in visceral adipose tissue.

In the livers of both Wistar and GK rats, all of the clock and clock-controlled genes examined (including clock) exhibited significant 24-h rhythmicity (Figure 3; $\chi^2 = 10.9–14.1$, each $P < 0.05$, Kruskal–Wallis test). As in the visceral adipose tissue, the rhythmic mRNA expression of most of the genes examined (clock, Bmal1, Cry1, and Dbp) was not attenuated in GK rats. However, the peak level and amplitude of oscillation of Per2 was significantly reduced in GK rats.

Discussion

Previous studies performed in our lab have revealed that peak transcription levels of clock genes are mildly attenuated in the visceral adipose tissue of obese KK mice and are greatly attenuated in that of more obese, diabetic KK-A^y mice compared to control C57BL/6J mice (11). In contrast, this study demonstrated that rhythmic mRNA expression of clock genes is not dampened in the visceral adipose tissue of nonobese diabetic GK rats. Given

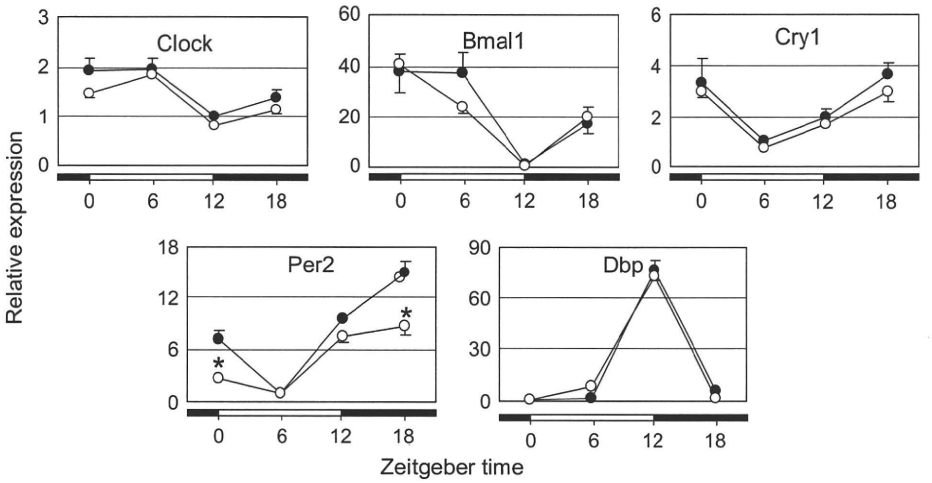

Figure 3. Daily mRNA expression profiles of clock genes in the liver of Wistar (●—●) and GK (○—○) rats. Data are reported as the means and SE of four rats at each time point and are expressed as relative values (compared to the lowest values in Wistar rats) for each gene. $*P < 0.05$ vs. Wistar rats.

that more than one clock gene is involved in the regulation of adipocyte differentiation (14,15), impairment of molecular clock function in the visceral adipose tissue may be related to obesity, but not directly to diabetes.

However, rhythmic mRNA expression of Per2 was mildly, but significantly, attenuated in the liver of GK rats. Kuriyama, Sasahara, Kudo, and Shibata (21) also reported that rhythmic Per2 expression is impaired in the liver, but not the SCN, of streptozotocin-induced, type 1 diabetic mice. In this model, treatment with insulin not only ameliorated hyperglycemia, but recovered impaired Per2 expression rhythms in the liver. These findings suggest that both type 1 and type 2 diabetes, even in the absence of obesity, could affect hepatic Per2 expression. Given that glucose can downregulate Per2 expression in Rat-1 fibroblasts *in vitro* (22), hyperglycemia may reduce peak mRNA levels of Per2 in the liver of diabetic animals.

In spite of the mild attenuation of Per2 expression, rhythmic mRNA expression of the other clock genes examined, and the representative clock-controlled gene Dbp, was not dampened in the liver of GK rats. These results seem to be consistent with findings suggesting that rhythmic Per1 expression is nearly normal in the SCN of heterozygous Per2 mutant mice, unlike in homozygous Per2 mutants (23). Moreover, it has recently been reported that hepatocyte-specific downregulation of Bmal1 expression has little influence on the rhythmic expression of Per2 in the liver of mice; however, the rhythmic expression of Per1, Rev-erbα, and Dbp is greatly attenuated (24). Therefore, hepatic expression of Per2, unlike Per1 and Rev-erbα, appears to be driven not only by the local molecular clock, but also by some other systemic cues. Again, further studies are needed to determine whether hepatic glucose concentrations regulate the rhythmic expression of Per2 in the liver.

In conclusion, the molecular clock was scarcely impaired in the visceral adipose tissue and liver of diabetic GK rats. Oishi, Kasamatsu, and Ishida (25) have also shown that the molecular clock function is preserved to a great extent in the liver, heart, and

kidney of mice with streptozotocin-induced insulinopenic diabetes. Because both GK rats and streptozotocin-treated mice are nonobese, molecular clock impairment in the peripheral tissues of obese diabetic animals seems to be caused by factors related to obesity or obese, type 2 diabetes, but not hyperglycemia. In this case, the mechanisms underlying the association between obese diabetes and molecular clock function remain to be elucidated. Additionally, it is possible that the impaired molecular clock is a cause, but not a consequence, of obese diabetes. Further studies are necessary to more fully clarify the role of the molecular clock in the development of obesity and type 2 diabetes.

Declaration of Interest

The authors report no conflicts of interest. The authors alone are responsible for the content and writing of the paper.

References

1. Lowrey PL, Takahashi JS. Mammalian circadian biology: Elucidating genome-wide levels of temporal organization. *Annu Rev Genomics Hum Genet* 2004;5:407–441.
2. Reppert SM, Weaver DR. Coordination of circadian timing in mammals. *Nature* 2002;418: 935–941.
3. Bunger MK, Wilsbacher LD, Moran SM, Clendenin C, Radcliffe LA, Hogenesch JB, Simon MC, Takahashi JS, Bradfield CA. Mop3 is an essential component of the master circadian pacemaker in mammals. *Cell* 2000;103:1009–1017.
4. Gekakis N, Staknis D, Nguyen HB, Davis FC, Wilsbacher LD, King DP, Takahashi JS, Weitz CJ. Role of the CLOCK protein in the mammalian circadian mechanism. *Science* 1998;280:1564–1569.
5. Kume K, Zylka MJ, Sriram S, Shearman LP, Weaver DR, Jin X, Maywood ES, Hastings MH, Reppert SM. mCRY1 and mCRY2 are essential components of the negative limb of the circadian clock feedback loop. *Cell* 1999;98:193–205.
6. Okamura H, Miyake S, Sumi Y, Yamaguchi S, Yasui A, Muijtjens M, Hoeijmakers JH, van der Horst GT. Photic induction of mPer1 and mPer2 in cry-deficient mice lacking a biological clock. *Science* 1999;286:2531–2534.
7. Vitaterna MH, Selby CP, Todo T, Niwa H, Thompson C, Fruechte EM, Hitomi K, Thresher RJ, Ishikawa T, Miyazaki J, Takahashi JS, Sancar A. Differential regulation of mammalian period genes and circadian rhythmicity by cryptochromes 1 and 2. *Proc Natl Acad Sci USA* 1999;96:12114–12119.
8. Panda S, Antoch MP, Miller BH, Su AI, Schook AB, Straume M, Schultz PG, Kay SA, Takahashi JS, Hogenesch JB. Coordinated transcription of key pathways in the mouse by the circadian clock. *Cell* 2002;109:307–320.
9. Storch KF, Lipan O, Leykin I, Viswanathan N, Davis FC, Wong WH, Weitz CJ. Extensive and divergent circadian gene expression in liver and heart. *Nature* 2002;417:78–83.
10. Yoo SH, Yamazaki S, Lowrey PL, Shimomura K, Ko CH, Buhr ED, Siepka SM, Hong HK, Oh WJ, Yoo OJ, Menaker M, Takahashi JS. PERIOD2:LUCIFERASE real-time reporting of circadian dynamics reveals persistent circadian oscillations in mouse peripheral tissues. *Proc Natl Acad Sci USA* 2004;101:5339–5346.
11. Ando H, Yanagihara H, Hayashi Y, Obi Y, Tsuruoka S, Takamura T, Kaneko S, Fujimura A. Rhythmic messenger ribonucleic acid expression of clock genes and adipocytokines in mouse visceral adipose tissue. *Endocrinology* 2005;146:5631–5636.
12. Stumvoll M, Goldstein BJ, van Haeften TW. Type 2 diabetes: principles of pathogenesis and therapy. *Lancet* 2005;365:1333–1346.
13. Turek FW, Joshu C, Kohsaka A, Lin E, Ivanova G, McDearmon E, Laposky A, Losee-Olson S, Easton A, Jensen DR, Eckel RH, Takahashi JS, Bass J. Obesity and metabolic syndrome in circadian Clock mutant mice. *Science* 2005;308:1043–1045.

14. Shimba S, Ishii N, Ohta Y, Ohno T, Watabe Y, Hayashi M, Wada T, Aoyagi T, Tezuka M. Brain and muscle Arnt-like protein-1 (BMAL1), a component of the molecular clock, regulates adipogenesis. *Proc Natl Acad Sci USA* 2005;102:12071–12076.
15. Fontaine C, Dubois G, Duguay Y, Helledie T, Vu-Dac N, Gervois P, Soncin F, Mandrup S, Fruchart JC, Fruchart-Najib J, Staels B. The orphan nuclear receptor Rev-Erbalpha is a peroxisome proliferator-activated receptor (PPAR) gamma target gene and promotes PPARgamma-induced adipocyte differentiation. *J Biol Chem* 2003;278:37672–37680.
16. Yamauchi T, Kamon J, Waki H, Murakami K, Motojima K, Komeda K, Ide T, Kubota N, Terauchi Y, Tobe K, Miki H, Tsuchida A, Akanuma Y, Nagai R, Kimura S, Kadowaki T. The mechanisms by which both heterozygous peroxisome proliferator-activated receptor gamma (PPARgamma) deficiency and PPARgamma agonist improve insulin resistance. *J Biol Chem* 2001;276:41245–41254.
17. Shima K, Ando H, Matsuzawa N, Takamura T, Fujimura A, Kaneko S. Influences of hyperglycemia, hyperinsulinemia, and hepatic steatosis on the circadian clock in mouse liver. *Diabetologia* 2007;50(suppl 1):S60.
18. Portha B. Programmed disorders of beta-cell development and function as one cause for type 2 diabetes? The GK rat paradigm. *Diabetes Metab Res Rev* 2005;21:195–504.
19. Homo-Delarche F, Calderari S, Irminger JC, Gangnerau MN, Coulaud J, Rickenbach K, Dolz M, Halban P, Portha B, Serradas P. Islet inflammation and fibrosis in a spontaneous model of type 2 diabetes, the GK rat. *Diabetes* 2006;55:1625–1633.
20. Ando H, Oshima Y, Yanagihara H, Hayashi Y, Takamura T, Kaneko S, Fujimura A. Profile of rhythmic gene expression in the livers of obese diabetic KK-A(y) mice. *Biochem Biophys Res Commun* 2006;346:1297–1302.
21. Kuriyama K, Sasahara K, Kudo T, Shibata S. Daily injection of insulin attenuated impairment of liver circadian clock oscillation in the streptozotocin-treated diabetic mouse. *FEBS Lett* 2004;572:206–210.
22. Hirota T, Okano T, Kokame K, Shirotani-Ikejima H, Miyata T, Fukada Y. Glucose down-regulates Per1 and Per2 mRNA levels and induces circadian gene expression in cultured Rat-1 fibroblasts. *J Biol Chem* 2002;277:44244–44251.
23. Zheng B, Larkin DW, Albrecht U, Sun ZS, Sage M, Eichele G, Lee CC, Bradley A. The mPer2 gene encodes a functional component of the mammalian circadian clock. *Nature* 1999;400:169–173.
24. Kornmann B, Schaad O, Bujard H, Takahashi JS, Schibler U. System-driven and oscillator-dependent circadian transcription in mice with a conditionally active liver clock. *PLoS Biol* 2007;5:e34.
25. Oishi K, Kasamatsu M, Ishida N. Gene- and tissue-specific alterations of circadian clock gene expression in streptozotocin-induced diabetic mice under restricted feeding. *Biochem Biophys Res Commun* 2004;317:330–334.

Diabetologia (2009) 52:329–335
DOI 10.1007/s00125-008-1194-6

ARTICLE

Clock gene expression in peripheral leucocytes of patients with type 2 diabetes

H. Ando · T. Takamura · N. Matsuzawa-Nagata · K. R. Shima · T. Eto · H. Misu · M. Shiramoto · T. Tsuru · S. Irie · A. Fujimura · S. Kaneko

Received: 11 July 2008 / Accepted: 7 October 2008 / Published online: 31 October 2008

Abstract
Aim/hypothesis Recent studies have demonstrated relationships between circadian clock function and the development of metabolic diseases such as type 2 diabetes. We investigated whether the peripheral circadian clock is impaired in patients with type 2 diabetes.
Methods Peripheral leucocytes were obtained from eight patients with diabetes and six comparatively young non-diabetic volunteers at 09:00, 15:00, 21:00 and 03:00 hours (study 1) and from 12 male patients with diabetes and 14 age-matched men at 09:00 hours (study 2). Transcript levels of clock genes (*CLOCK*, *BMAL1* [also known as *ARNTL*], *PER1*, *PER2*, *PER3* and *CRY1*) were determined by real-time quantitative PCR.
Results In study 1, mRNA expression patterns of *BMAL1*, *PER1*, *PER2* and *PER3* exhibited 24 h rhythmicity in the leucocytes of all 14 individuals. The expression levels of these mRNAs were significantly ($p<0.05$) lower in patients with diabetes than in non-diabetic individuals at one or more time points. Moreover, the amplitudes of mRNA expression rhythms of *PER1* and *PER3* genes tended to diminish in patients with diabetes. In study 2, leucocytes obtained from patients with diabetes expressed significantly ($p<0.05$) lower transcript levels of *BMAL1*, *PER1* and *PER3* compared with leucocytes from control individuals, and transcript expression was inversely correlated with HbA_{1c} levels ($\rho=-0.47$ to -0.55, $p<0.05$).
Conclusions/interpretation These results suggest that rhythmic mRNA expression of clock genes is dampened in peripheral leucocytes of patients with type 2 diabetes. The impairment of the circadian clock appears to be closely associated with the pathophysiology of type 2 diabetes in humans.

Keywords Biological clock · Circadian rhythm · Clock gene · Type 2 diabetes

Abbreviations

BMAL1	brain and muscle Arnt-like protein 1
CLOCK	clock homologue (mouse)
HOMA-IR	homeostasis model assessment for insulin resistance
SCN	suprachiasmatic nucleus

Introduction

The circadian system is responsible for regulating a variety of physiological and behavioural processes, including

Electronic supplementary material The online version of this article (doi:10.1007/s00125-008-1194-6) contains supplementary material, which is available to authorised users.

H. Ando (✉) · A. Fujimura
Division of Clinical Pharmacology, Department of Pharmacology, School of Medicine, Jichi Medical University,
3311-1 Yakushiji, Shimotsuke,
Tochigi 329-0498, Japan
e-mail: h-ando@jichi.ac.jp

H. Ando · T. Takamura · N. Matsuzawa-Nagata · K. R. Shima · H. Misu · S. Kaneko
Department of Disease Control and Homeostasis, Kanazawa University Graduate School of Medical Science, Kanazawa, Japan

T. Eto · M. Shiramoto · T. Tsuru
PS Clinic, Medical Co. LTA,
Fukuoka, Japan

S. Irie
LTA Clinical Pharmacology Center, Medical Co. LTA,
Fukuoka, Japan

feeding behaviour and energy metabolism [1, 2]. Recent studies revealed that the circadian clock system consists essentially of a set of clock genes [1, 2]. The circadian clock resides in the hypothalamic suprachiasmatic nucleus (SCN), which is recognised as being the master clock, and the same clock exists also in almost all peripheral tissues, including liver, heart, kidney [3–5] and leucocytes [6–8]. Although the SCN is not essential for driving peripheral oscillations, it appears to coordinate peripheral clocks [5].

In mammals, rhythmic transcriptional enhancement by two basic helix–loop–helix transcription factors, clock homologue (mouse) (CLOCK) and brain and muscle Arnt-like protein 1 (BMAL1), provides the basic drive for the intracellular circadian clock (Electronic supplementary material [ESM] Fig. 1) [9, 10]. The heterodimer activates the transcription of several other clock genes, including those for period (PER) and cryptochrome (CRY) [11–13]. The resultant PER and CRY proteins heterodimerise, translocate to the nucleus, and inhibit the activity of CLOCK–BMAL1, thus forming a transcriptional–translational feedback loop. In parallel, the CLOCK–BMAL1 heterodimer activates the transcription of various clock-controlled genes [1, 2]. Given that some clock-controlled genes also serve as transcription factors, the expression of numerous genes may be tied to the functions of the circadian clock [1, 2]. Moreover, nearly half of the known nuclear receptors, including peroxisome proliferator-activated receptors (α, γ and δ) and thyroid hormone receptors (α and β), exhibit circadian expression in the liver and adipose tissues, providing an explanation for the cyclic behaviour of glucose and lipid metabolism [14].

Recently, the link between circadian clock function and metabolic diseases has attracted attention. Turek et al. [15] demonstrated that *Clock* mutant mice are hyperphagic and develop metabolic syndrome, hyperglycaemia and hyperlipidaemia. In addition, we showed that the rhythmic expression of clock genes is blunted in the liver and visceral adipose tissues of KK-A^y mice, a genetic model of type 2 diabetes [16]. In humans, genetic variations in the *BMAL1* gene (also known as *ARNTL*) are reported to be associated with susceptibility to type 2 diabetes and hypertension [17]. Furthermore, *CLOCK* haplotypes are associated with metabolic syndrome [18] and non-alcoholic fatty liver disease [19]. These findings strongly indicate that dysfunction of the circadian clock contributes to the development of type 2 diabetes and metabolic syndrome. However, whether clock function is impaired in human patients with these metabolic diseases, as has been shown in mice, remains to be determined. To address this issue, we obtained peripheral leucocytes from patients with type 2 diabetes and from non-diabetic volunteers and compared their mRNA expression rhythms of clock genes.

Methods

Participants Studies 1 and 2 were approved by the ethics committees of Kanazawa University (Kanazawa, Japan) and Medical Co. LTA (Fukuoka, Japan), respectively, and were conducted in accordance with the Declaration of Helsinki as revised in 2000. All individuals were Japanese and participated in the study after giving their written informed consent. We excluded the following individuals: those who had experienced either jet lag or shift work during the 2 weeks preceding the study, those who took psychotrophic drugs in the preceding month, and those with sleep disorder, inflammatory disease, malignancy or anaemia. Additional information about the lifestyles (habits, mealtimes and sleep time) was collected from all participants on the day of the study.

Study 1 The first study was performed from October to December 2006. Eight inpatients with type 2 diabetes and two non-diabetic inpatients with fatty liver were recruited from Kanazawa University Hospital (Kanazawa). All patients with diabetes met the American Diabetes Association's diagnostic criteria for diabetes [20], whereas the other two were classified as having normal glucose tolerance and impaired fasting glucose, respectively, based on a 75 g OGTT. Four healthy men were also enrolled in this study. All of the 14 individuals kept regular hours for at least 2 weeks until the study day or hospital admission. Most individuals usually had three meals a day, whereas one healthy individual always skipped breakfast (ESM Fig. 2). As shown in Table 1, fasting glucose and HbA_{1c} levels in patients with diabetes were significantly higher than those in non-diabetic individuals. In six of eight patients with diabetes, the disease was poorly controlled ($HbA_{1c} \geq 7.0\%$). Three of the six patients were treated with oral agents (pioglitazone, glimepiride + metformin and glibenclamide + metformin + acarbose, respectively). Additionally, patients with diabetes were older than the non-diabetic individuals. The other variables did not differ between the groups.

On the day of the study, blood samples were taken from the forearm vein at 09:00, 15:00, 21:00 and 03:00 hours beginning at 09:00 hours. We chose these time points because *BMAL1* and *PER2* mRNA levels have been reported to peak at about 15:00 and 08:00 hours, respectively [21]. The healthy individuals were asked to assume their everyday routines and sleep in a dim room at their usual times. For the inpatients, sampling commenced within 48 h after admission and was conducted in their hospital room. Fasting blood samples for clinical chemistry were obtained from the inpatients in the early morning on the day after the admission and from the healthy individuals at least 2 weeks before the study day.